



A new framework for evaluating and enhancing the performance of district heating systems integrated with data centres using short-term thermal energy storage

Han Du ^a, Xinlei Zhou ^a, Natasha Nord ^b, Yale Carden ^c, Ping Cui ^d, Zhenjun Ma ^{a,*}

^a Sustainable Buildings Research Centre, University of Wollongong, NSW, 2522, Australia

^b Department of Energy and Process Engineering, Norwegian University of Science and Technology, Norway

^c Geoxchange Australia PTY Ltd., North Sydney, NSW, 2060, Australia

^d School of Thermal Engineering, Shandong Jianzhu University, Jinan, 250101, Shandong, China

ARTICLE INFO

Handling Editor: Q. F. Ofelia Araujo

Keywords:

District heating
Data centres
Thermal energy storage
Performance evaluation
Energy flexibility

ABSTRACT

This paper proposes a new framework to assess and enhance the performance of district heating (DH) systems integrated with data centres (DCs). This framework utilizes six key performance indicators tailored specifically for DH and DC hybrid systems to evaluate energy flexibility, energy efficiency, and operational cost savings. To further enhance system flexibility, a dual short-term thermal energy storage (TES) solution is proposed, enabling peak shaving and load shifting of the hybrid system through price-driven and demand-driven strategies, supported by a hybrid global optimization algorithm. A parametric study is also carried out to investigate the impact of water tank size on system performance across a wide range of energy storage scenarios. A case study of a DH and DC hybrid system in Norway demonstrated the effectiveness of the framework in capturing the performance characteristics of the hybrid system. This study showed that incorporating dual water tanks and the proposed energy management strategies achieved a 2.1 % increase in the load shifting ratio, a 10 % increase in the peak demand reduction ratio, and a 3.2 % decrease in the total operational cost. The parametric analysis revealed that larger TES sizes increased peak shaving capacity and cost reduction, albeit with minimal impact on load shifting capacity.

Nomenclature

COP	coefficient of performance
DC	data centre
DH	district heating
DHW	domestic hot water
e_i	the spot price from the power market
\dot{E}_i	the rate of electricity use
E_i	the integral electricity demand
f_{sur}	heating peak demand price
f_{ren}	grid rent price of electricity cost
F	the fixed fee of electricity cost
HE_i	heating demand price
P_{ene}	the cost of heating demand
P_{ele_mon}	electricity costs for one month
P_{hea_mon}	total heating costs for one month
P_{sur}	the cost of peak heating demand
P_{total_mon}	the total operational cost for one month

(continued on next column)

(continued)

\dot{Q}_{co}	the rate of cooling energy generated by heat pumps for the data centre
\dot{Q}_i	heating rate supplied to end users
\dot{Q}_{hd}	current-step heating demand
\dot{Q}_{sur}	the average peak heating demand during the three highest-demand hours
\dot{Q}_{wa}	the rate of waste heat generated by heat pumps and the data centre
R2R	return-to-return
R2S	return-to-supply
RES	renewable energy source
TES	thermal energy storage
v_{ld}	the water flow distribution ratio for load shifting
v_{ps}	the water flow distribution ratio for peak shaving
W_{con}	the rate of electricity use of heat pumps

1. Introduction

In the past few years, the concept of energy flexibility in district

* Corresponding author.

E-mail address: zhenjun@uow.edu.au (Z. Ma).

heating (DH) systems has emerged as a critical solution to reduce traditional fossil fuel reliance and mitigate the environmental impact [1, 2]. Transitioning to renewable energy sources (RESs) and the integration of waste heat recovery introduce stability concerns but also bring significant environmental benefits [3]. This transition is particularly relevant in the building sector, where space air conditioning and domestic hot water (DHW) are among the major energy consumers, often relying directly on primary energy sources [4]. Therefore, evaluating the operational performance and enhancing the energy flexibility of DH systems are essential to reduce energy use, decrease greenhouse gas emissions, and advance sustainable development.

The thermal piping networks of DH systems, dating back to the 19th century, have evolved significantly [5]. The first three generations relied on extensive steam and hot water for heating, which suffered from substantial thermal energy losses due to their high supply temperatures of 100 °C or above [6]. In contrast, the 4th generation DH systems lowered hot water supply temperatures to 70 °C or even 50 °C, drastically cutting down heat loss and facilitating the integration with RESs or waste heat recovery technologies to enhance the operating efficiency [6, 7]. Building on this innovation, the 5th generation DH systems can operate efficiently at temperatures near ambient temperature (e.g., 15–25 °C), simultaneously meeting both heating and cooling requirements through ultra-low temperature networks [8–11].

Various energy technologies can be integrated into DH systems and the integrated systems have shown great potential for improved efficiency and considerable energy savings [12]. A key advancement in energy efficiency and conservation is achieved by integrating waste heat recovery from data centres (DCs) into DH systems [13–16]. For instance, a 100 kW non-integrated DC generated 926 MWh/year of waste heat, contributing to the urban heat island effect. If integrated into a DH system, this waste heat can supply 12–59 % of the energy demand and reduce gas consumption by 11–58 %, depending on the capacities of the DCs [17]. A study in Finland, which utilized real plant data and DH heating demand from 2013 to 2015, revealed that incorporating 20–60 MW waste heat into a DH network with a load varying between 50 and 780 MW can decrease the operational costs by 0.6–7.3 % [18]. Another study indicated that DCs in Latvia produced 51.37 GWh of waste heat in 2022, and this number could rise to 257 GWh by 2050, among which 201 GWh of waste heat can be potentially used for heating [19]. By using a composite performance metric, including the amount of waste heat, the coefficient of performance (COP) of heat pumps, and the quality of waste heat, Du et al. [20] discovered the effects of waste heat reuse on DH networks via data mining technologies. Oró et al. [21] explored air-cooled DCs and it was found that integrating heat recovery in a conventional air-cooled data centre with 1000 kW capacity achieved a primary energy reuse rate above 50 %, although the economic feasibility was often not viable when considering the initial investments. The above studies highlighted that DCs can produce a substantial quantity of waste heat, and significant heating energy savings can be achieved by incorporating the waste heat recovery into DH systems.

In addition to incorporating waste heat recovery, enhancing the energy flexibility of DH systems is also essential for increased operating efficiency and resilience. Energy flexibility relies on the network itself [22,23], building thermal inertia [24], and thermal energy storage (TES) used [25,26]. For example, a case study on residential buildings supplied with heating energy by a DH network in Copenhagen showed that utilizing building thermal mass as heat storage could significantly reduce the peak load by 40–87 % through aligning heating schedules with energy prices [27]. Another study in the same region showed that employing building thermal mass as heat storage in buildings connected to the DH network effectively shifted the heating load by 41–51 %, without compromising indoor thermal comfort [28]. Additionally, DH networks enabled peak shaving by pre-loading with varying temperatures, reducing later instantaneous heating demand. However, frequent higher or lower temperatures can accelerate material fatigue, particularly in steel pipes, leading to the quick development of cracks [4].

Furthermore, TES plays a significant role in enhancing the energy flexibility of DH systems, encompassing both short-term and long-term (seasonal) solutions [29]. Typically, for daily operations, most systems predominantly used sensible heat storage, such as water tanks. For longer periods, covering weekly and seasonal cycles, storage was frequently employed in solar-heated DH systems [30]. Olsthoorn et al. [31] conducted a review of the models and applications of various TES systems, with a particular focus on the integration of RESs with DH networks. Another study [32] demonstrated that incorporating a water tank into DH systems integrated with DCs (named as hybrid DH systems hereafter) can effectively utilize waste heat to mitigate the supply-demand mismatch in the non-heating season and enhance energy flexibility by reducing peak demand during the heating season. Pans et al. [33] investigated net-zero DH systems utilizing RESs (i.e., solar, geothermal, and wind) with decentralized and centralized TES to match heat generation with demand, and also evaluated how the temperature of TES affects system costs and efficiency. The results showed that the average minimum cost per dwelling (i.e., 282 dwellings in total) was £12,278 with an energy efficiency of 84.84 % when using a 15,000 m³ centralized tank at 60 °C by tuning wind and PV capacities to fulfill hourly heating demand. Li et al. [34] integrated two TES approaches, including a water tank for short-term needs, capable of reducing peak load by 31 % and energy costs by 5 %, and a borehole TES system for long-term use, which could enhance waste heat utilization rate from 77 % to 96 % and cut CO₂ emissions by 8 % annually. Miedaner et al. [35] detailed the practical implementation of a borehole TES system in two DH systems in Germany and Denmark. Romanchenko et al. [36] explored the effects of integrating demand-side flexibility via indoor temperature adjustments and supply-side flexibility via a seasonal pit TES in DH systems. The results indicated that combining demand-side flexibility with centralized TES can reduce overall space heating demand and operating costs of DH systems while the presence of supply-side TES lessened the impact of demand response. The above findings underscored the importance of TES to improve energy flexibility of DH systems and showed significant advantages of enhancing overall system performance and sustainability. Advanced TES technologies, such as pumped TES [37], and compressed air energy storage [38], have also been investigated, showing further opportunities for innovations in the field.

In addition, previous research has preliminarily explored operational strategies to enhance the energy flexibility of DH systems. For instance, Péan et al. [39] employed a rule-based control strategy to boost building energy flexibility by establishing low and high electricity price thresholds, derived from the 40th and 60th percentiles of the ahead prices. The temperature setpoints for space heating and DHW supply were adjusted by ±1 °C and ±5 °C respectively when these thresholds were exceeded. This strategy resulted in a 22–26 % cost reduction and a 2–4% rise in energy usage, while maintaining acceptable comfort levels. Sophisticated algorithms like Model Predictive Control have also been investigated to optimize the charging and discharging of TES to minimize the operational costs of DH systems [40,41]. It was shown that effective operational strategies can significantly improve the energy flexibility of DH systems, leading to cost savings.

From the above analysis, it can be concluded that hybrid DH systems can significantly enhance energy efficiency, reduce operational costs, and improve environmental sustainability. While existing research has predominantly evaluated such systems from energy, economic, and environmental perspectives, there remains a notable gap in the literature regarding the assessment of the performance of hybrid DH systems incorporating energy flexibility indicators. Moreover, most existing studies have focused primarily on either peak shaving or load shifting using single short-term thermal storage solutions to reduce the operational costs of hybrid DH systems, but few have specifically focused on enhancing energy flexibility by simultaneously addressing peak shaving and load shifting through short-term TES solutions, coupled with the consideration of day-ahead spot pricing.

Consequently, this study aims to evaluate and enhance the energy flexibility of hybrid DH systems, with a focus on both load shifting and peak shaving by using short-term TES systems. The main novelties of this study include: 1) dual short-term thermal energy storage systems were introduced to improve the energy flexibility of hybrid DH systems, facilitating both peak shaving and load shifting; 2) a hybrid global optimization algorithm integrated with rule-based control strategies, i.e., momentary control and moving average control, was tailored for dual TES systems, in which the global optimization algorithm was used to optimize the parameter settings used in the rule-based strategies; and 3) a multi-dimensional performance analysis incorporating multiple flexibility indicators was carried out to evaluate the performance of the hybrid DH systems, taking into account the changes in energy flexibility and the interactions among different performance indicators. This framework can act as a valuable reference for developing and managing hybrid DH systems, enhancing energy flexibility, and reducing operational costs.

2. New framework development

2.1. Outline of the framework

Fig. 1 outlines the proposed framework, which mainly consists of: i) a multi-dimensional performance analysis with flexibility indicators, ii) the development of TES solutions (i.e., water tanks) to improve system flexibility by using rule-based strategies integrated with a hybrid global optimization algorithm for efficient tank management, and iii) scenario analysis and evaluation.

Following a detailed analysis of the operational characteristics of hybrid DH systems, several key performance indicators were first selected and these indicators include the waste heat contribution ratio, cost savings ratio, COP change ratio, peak reduction ratio, electricity cost change ratio, and load shifting ratio. Next, a performance radar chart that incorporates these indicators was created to illustrate the overall performance of the system. In the second step, two hot water tanks which were used as short-term TES respectively for peak shaving

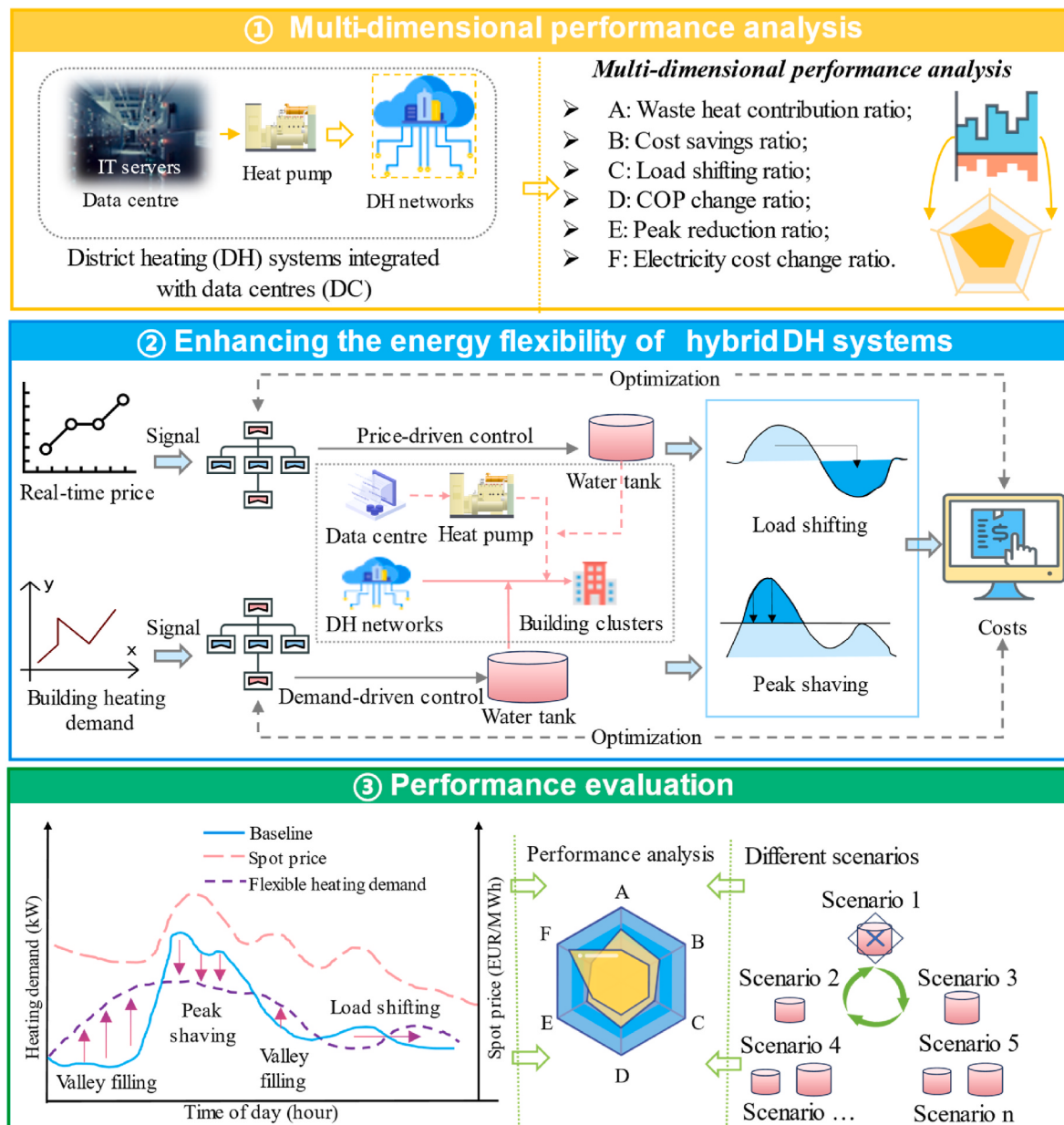


Fig. 1. Outline of the framework.

and load shifting were integrated with the DH systems to enhance energy flexibility. Peak shaving is influenced by the peak in the heating demand of buildings, while load shifting depends on electricity or heating spot prices. Due to the fundamental difference between the two approaches, a single tank may not effectively achieve both objectives, even with a well-designed control strategy. Two rule-based control strategies, including moving average and momentary control, were then developed to charge and discharge heat from the water tanks to facilitate load shifting and peak shaving, respectively. A global optimization algorithm was used to optimize the parameter settings for the rule-based strategies. The effectiveness of the proposed framework was assessed through a case study in Norway, using simulations conducted with TRNSYS. Lastly, various scenarios that considered configurations with one water tank and two water tanks governed by different rule-based control strategies were designed and evaluated using distinct performance radar maps. Additionally, the impact of the size of the water tanks on the overall system performance was analyzed.

2.2. Performance indicators for multi-dimensional evaluation

Considering the characteristics of DH systems integrated with DCs, as well as insights from previous studies, including historical data analysis [20] and electricity-related research [42]. Six indicators were selected to assess the operational performance and capture the characteristics of the hybrid DH systems.

- Cost savings ratio: it is the ratio of cost savings of a scenario to the total cost of a baseline scenario. It is used to assess the economic efficiency of the DH systems.
- Load shifting ratio (heating demand cost savings ratio): it is the ratio of cost savings of heating demand in a scenario to the total heating demand of a baseline scenario. This indicator is associated with the amount of heating energy used and the dynamic pricing of heating energy and does not consider the cost of peak load surcharges. When TES is introduced to facilitate load shifting, it can also be used to measure the extent to which energy use is shifted from peak price periods to off-peak periods.
- Peak reduction ratio: it is the ratio of the peak reduction of heating demand in a scenario to the peak demand of a baseline scenario. Peak shaving involves reducing heating demand during peak demand periods, effectively flattening the demand curve. Waste heat reuse, renewable energy integration, and TES can reduce the peak demand.
- COP change ratio: it is the ratio of the change in the average COP of the heat pumps in a scenario to that of a baseline scenario. In this study, the COP is related to the cooling energy generation rate, waste heat utilization rate, and the electrical power use of the heat pumps, and is calculated by Eq. (1).

$$COP = \frac{(\dot{Q}_{co} + \dot{Q}_{wa})}{\dot{W}_{con}} \quad (1)$$

Where \dot{Q}_{co} represents the rate of cooling energy generated by heat pumps and supplied to DCs, \dot{Q}_{wa} denotes the rate of waste heat generated by heat pumps for preheating water, and \dot{W}_{con} is the rate of electricity used by heat pumps.

- Load covering ratio (waste heat contribution ratio): it is the ratio of the quantity of the waste heat recovered from the DC to the total building heating demand during the same time period. It demonstrates the percentage of waste heat contribution towards meeting building heating demand. The value of this indicator is influenced by the capacity of the DC and building heating demand.
- Electricity costs change ratio: it is the ratio of the change (increase or decrease) in electricity costs of a scenario to the electricity costs of a baseline scenario. This indicator reflects the variation in electricity

costs to evaluate the impact of incorporating waste heat recovery or operational strategies on electricity cost savings.

A radar chart, incorporating the above indicators, was utilized to represent the overall performance of the hybrid DH systems.

2.3. Enhancing the energy flexibility of hybrid district heating systems

2.3.1. District heating price and electricity price model

The dynamic electricity pricing models used in previous studies include critical peak pricing, time-of-use pricing, and real-time pricing [43]. Critical peak pricing targets a few high-demand periods of a year with significantly higher prices to encourage end users to reduce their energy use. Time-of-use pricing segments the day into several periods with different prices reflecting typical demand levels, encouraging end users to shift use from peak demand periods to off-peak times. Real-time pricing (spot pricing) is the most dynamic one, which adjusts the prices frequently (hourly), based on real-time supply and demand, offering consumers the opportunity to use electricity when it is less expensive [43,44].

In Norway, approximately 65 % of the electricity supplied to the market is subject to dynamic pricing, which is based on spot prices and hourly metering [45]. Consequently, in this study, the spot price for electricity (real-time pricing) was used. It is commonly observed that the price variation of DH systems is regulated to align with the electricity prices [46]. Therefore, in this study, both electricity and heating spot prices were sourced from a single energy provider to ensure reliability [47]. It is noteworthy that while the spot prices for electricity are the same as those for heating, the pricing models, taxes, and coefficients applied to heating and electricity are different.

A detailed discussion of a generalized heating price model can be found in Ref. [32]. This heating price model primarily focused on the energy demand and the peak load demand components, as they are most frequently incorporated in existing heating pricing strategies. The energy demand component was used to cover the fuel costs according to the total heat use of end users. Conversely, the peak load demand component was used to maintain the necessary capacity for peak loads based on the peak heating demand. In this study, the following DH price model was used by referring to Ref. [48].

$$P_{hea_mon} = P_{ene} + P_{sur} \quad (2)$$

$$P_{ene} = \int_{t_0}^{t_f} HE_i \cdot \dot{Q}_i \cdot dt \quad (3)$$

$$P_{sur} = f_{sur} \cdot \dot{Q}_{sur} \quad (4)$$

where P_{hea_mon} represents the total heating costs for one month, P_{ene} denotes the costs of heating energy demand, which is linked to the day-ahead spot price, and P_{sur} represents the costs of peak load demand associated with the peak of heating demand, HE_i is the heating energy demand price, calculated as the spot price from the power market plus any applicable taxes (i.e., 0.2294 EUR), \dot{Q}_i is the heating rate supplied to end users, f_{sur} is the heating peak load demand price (i.e., 3.8 EUR/kW/month), and \dot{Q}_{sur} is the average of the three highest hours representing the monthly peak heating demand, according to Ref. [49].

Several European countries are using the electricity price model similar to that outlined in Eq. (5), which consists of the grid rent fees, taxes, and a variable market price [50]. In certain instances, a surcharge for high peak load is also applied.

$$P_{ele_mon} = (1 + 0.25) \cdot \int_{t_0}^{t_f} \dot{E}_i \cdot e_i \cdot dt + f_{ren} \cdot E_i + \frac{F}{12} \quad (5)$$

where P_{ele_mon} represents the monthly electricity costs, f_{ren} is a grid rent price set at 0.023 EUR/kWh in this study, \dot{E}_i indicates the electricity use

rate, E_i is the integral electricity demand, e_i is the spot price from the power market, and F represents the fixed fee of 190 EUR/year [50,51].

In this study, heating use is significantly larger than electricity use, and therefore, the surcharge fee for the high peak load of electricity is ignored. The total system cost is the sum of both electricity and heating costs for a month.

2.3.2. Enhancing energy flexibility through short-term thermal energy storage

Short-term TES is a prevalent method for enhancing system flexibility, enabling the adjustment and management of the energy demand profile. It can assist in achieving load shifting and peak shaving. In DH systems, load shifting refers to the strategy of adjusting the timing of heating usage to utilize off-peak heating pricing hours, which can reduce heating costs. This strategy is driven by heating pricing signals such as day-ahead spot pricing. However, due to the uncertainty and fast dynamics between valley-price and peak-price periods, achieving load shifting under spot pricing needs fast charging of TES during short low-price windows before the price increases, and then fast discharging during short high-price windows before the price decreases. Conversely, in DH systems, peak shaving refers to the strategy of reducing the maximum heating demand during peak usage periods, which helps stabilize the thermal grid and reduce load demand surcharge costs. However, to achieve peak shaving, TES needs to be continuously charged to ensure that a sufficiently high temperature and adequate heat are available before peak demand appears, thereby helping reduce peak surcharge costs.

In this study, to improve the flexibility of the hybrid DH system, two TES systems (i.e., hot water tanks) were incorporated into the hybrid DH system. One water tank was employed for peak shaving based on building heating demand, while the other one was used to facilitate heating load shifting driven by spot prices. Given the different trends of price and heating demand, the dual tank setup was considered in this study.

Fig. 2 illustrates the configuration and operation of dual TES systems. Building return water was split into two streams. One stream is flowing directly through the water tank for load shifting based on spot prices and the tank is heated by the waste heat recovered from the DC. The second stream is mixed with the pre-heated water and after mixing, it is then divided into two new streams again. One stream of the mixture passes through the water tank for peak shaving based on momentary heating demand, and the tank is heated by one of the two heat exchangers in the DH substation. The other stream is mixed again with the heated water, and the mixture is then heated by the second heat exchanger to the required heating temperature for space heating. Please note that the water flow distribution ratio (i.e. v_{ld} and v_{ps}) was optimized in this study.

In a previous study [32], the impact of different tank sizes on heat usage was analyzed, providing a foundational reference for this study. Based on these findings, a tank size of 900 m³ was selected for peak shaving and 600 m³ for load shifting. The initial capacity of the water tank for load shifting was set at 600 m³ and was further refined through trial-and-error testing. This capacity differed from the tank used for peak

shaving. This distinction arose because load shifting required rapid charging of the water tank to reach the desired temperature during the low-price periods, followed by discharging during the high-price periods. Therefore, a relatively smaller water tank was sufficient due to frequent charging or discharging cycles. The tank was charged by the waste heat recovered from DCs. Conversely, the peak shaving tank initially used was 900 m³ and was further refined through trial-and-error testing. Compared to the tank for load shifting, the peak shaving tank required a relatively larger size as more heat is required to reduce the peak demand to charge sufficient heat into the tank for peak shaving. To avoid the effects of the high temperature on the COP of the heat pumps, this tank was charged via one of the two heat exchangers in the DH substation and the charging was completed when the average temperature in the tank reached its limit.

To analyze how the sizes of the water tanks affect system performance, a parametric study was conducted in this study. The considered capacities of the tank for peak shaving were 600 m³, 900 m³, 1200 m³, and 1500 m³, respectively, while those for load shifting were 300 m³, 600 m³, 900 m³, and 1200 m³, respectively. It is noted that all other parameters remained unchanged.

Besides the significance of the water tank size, control strategies also play a crucial role. Some basic rule-based control strategies typically used for district heating control are unable to respond effectively to dynamic spot prices [52], as spot prices show strong fluctuations and uncertainties in price variations. In this study, a moving average control strategy [53,54] was developed to capture the local patterns of the spot prices and manage the charging/discharging of a water tank, which allows for better adaptation to price fluctuations. This control logic operates as follows. If the current spot price exceeds the moving average of future n-hour spot prices and the temperature of the return water from buildings is less than that of the water tank, or the average temperature of the tank exceeds its limit, the heat in the water tank is discharged to heat the buildings. Otherwise, the tank is charged using the waste heat recovered from the DC. In this study, the future n-hour was set to 15 h ahead after trial-and-error testing, and the temperature limit of the tank for load shifting was set at 80°C.

In the meanwhile, a momentary control algorithm [53,54] was utilized to regulate the heat charging and discharging of the water tank for peak shaving. This algorithm determines whether to facilitate peak shaving by comparing the instantaneous building heating demand with a predetermined value, using the following rules. If the current heating demand does not exceed the predetermined value, the tank will be charged by one of the two heat exchangers until the average temperature of the tank reaches its upper limits. If the current heating demand exceeds the predetermined value, the heat will be discharged from the tank until the average temperature of the tank reaches its lower limit. This is different from the tank used for load shifting, where heat is sourced from the waste heat of the DC. Since the DC continuously produces waste heat and requires cooling energy, the load-shifting tank can keep charging and discharging cycles. Otherwise, the tank temperature would increase, affecting both the COP of the heat pumps and the cooling energy required by the DC. Conversely, the tank for peak

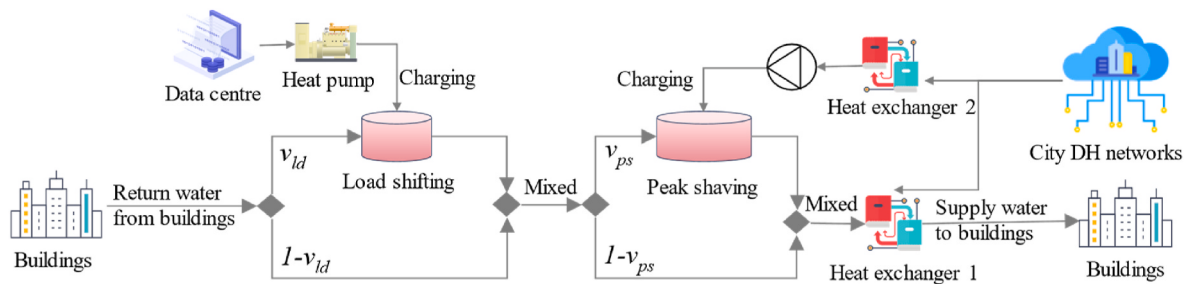


Fig. 2. Configuration and operation strategy of DH systems with the dual TES systems (v_{ps} refers to the water flow distribution ratio for peak shaving and v_{ld} refers to the water flow distribution ratio for load shifting).

shaving will stop charging once the desired temperature is achieved.

Fig. 3 illustrates how the heating demand can be modulated by using TES. In this example, the heating load profile was managed by two different approaches, including peak shaving and load shifting, which can be achieved by using energy flexible sources such as short-term TES (hot water tanks). The control signal was derived from the instantaneous heating demand and the spot prices, as described previously. In this study, the hot water tanks were utilized to enhance the energy flexibility of the hybrid DH system.

2.4. Evaluating the proposed framework via simulations

In this study, the dynamic operation of the hybrid DH systems was simulated using TRNSYS. The major component models selected for simulation are detailed in **Table 1**. Notably, the water-to-water heat pump model, functioning as a variable frequency heat pump, was custom-programmed and its validity was supported by previous literature [55]. The building heating demand and cooling energy demand of the DC were the actually measured data obtained from a case study to be presented in Section 3. Models for water tanks, water pumps, and controllers used were sourced from the standard TRNSYS library. The rated performance of the equipment used in this study is presented in **Table 2**. It was assumed that heat loss from the water tanks was neglected for the purposes of this study. This assumption simplified the analysis so the focus was concentrated on evaluating the performance of the framework under ideal conditions.

GenOpt is a Java-based optimization program for minimizing the cost objective function [56]. The TRNOPT interface component of TRNSYS facilitates the connection to the external optimization tool GenOpt [57]. The optimization process is shown in **Fig. 4**. By combining TRNSYS and GenOpt, GenOpt reads the deck (.dck) file generated by TRNSYS and automatically performs the optimization in the TRNSYS program. As described in **Fig. 2**, the variables v_{ps} and v_{ls} were important for determining the charging or discharging of TES.

The ratios of the water flow rate for peak shaving and load shifting in the rule-based control strategies are determined using Eq. (6)-Eq. (10), which can determine the heating charging and discharging of water tanks.

$$v_{ps} = \begin{cases} 0, & \dot{Q}_{hd} \leq b \\ a, & \dot{Q}_{hd} > b \end{cases} \quad (6)$$

where v_{ps} is the water flow distribution ratio of the flow for peak shaving to the total flow, optimized in the range of 0–1, a represents a coefficient, \dot{Q}_{hd} denotes the current-step heating demand, and b is the threshold of building heating demand.

$$v_{ld} = \begin{cases} 0, & Con \leq 0 \\ c, & Con > 0 \end{cases} \quad (7)$$

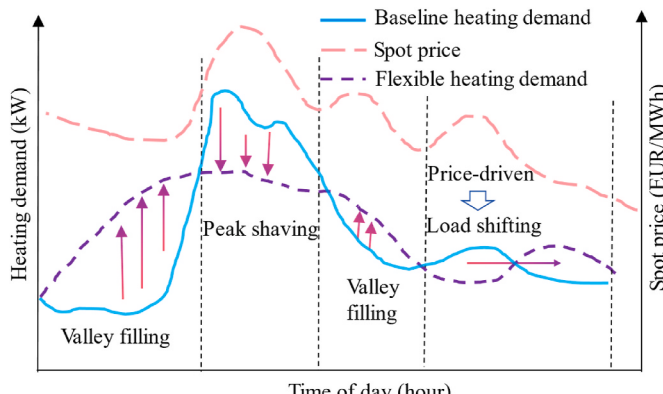


Fig. 3. An example of flexible heating demand management.

Table 1
Major component models used in TRNSYS simulation.

No.	Type	Function
1	Type 9e	Model for reading the heating demand of buildings, the cooling energy demand of the DC, and the spot prices
2	Type 682	Model for simulating ideal air conditioning
3	Type 225	Water-to-water heat pump
4	Type 4c	Thermal energy storage (hot water tank)
5	Type 114	Single-speed pump

Table 2
Rated parameters of the equipment used in this study.

Equipment	Specifications
Heat pump	Rated cooling capacity: 556 kW, rated heating capacity: 500 kW, rated cooling COP: 6, rated heating COP: 5, water flow: 88,000 kg/h, and designed chilled water outlet temperature: 7.5 °C.
Water pumps (DC side)	Rated flow rate: 88,000 kg/h, rated power: 16 kW, overall pump efficiency: 0.6, and motor efficiency: 0.9.
Other water pumps	Rated flow rates: 300,000 kg/h for the user side water pump and 88,000 kg/h for the water pump connected to the peak shaving water tank.
Water tank 1	Tank volume is 600 m ³ .
Water tank 2	Tank volume is 900 m ³ .

$$Con = \begin{cases} sig_{ld}, HE_i < d + \frac{\sum_{i=1}^{i=n} HE_i}{n} \\ sig_{ld} + sig_{ld}, HE_i \geq d + \frac{\sum_{i=1}^{i=n} HE_i}{n} \end{cases} \quad (8)$$

$$sig_{ld} = \begin{cases} 1, T_a - T_{limit} > DT_{upper1} \text{ and } sig_{ld}^{pre} = 0 \\ T_a - T_{limit} < DT_{lower1} \text{ and } sig_{ld}^{pre} = 1 \\ 0, \text{Otherwise} \end{cases} \quad (9)$$

$$sig_{ld} = \begin{cases} 1, T_a - T_{return} > DT_{upper2} \text{ and } sig_{ld}^{pre} = 0 \\ T_a - T_{return} < DT_{lower2} \text{ and } sig_{ld}^{pre} = 1 \\ 0, \text{Otherwise} \end{cases} \quad (10)$$

where v_{ld} is the water flow distribution ratio of the flow for load shifting to the total flow, which is to be optimized and is in the range of 0–1, c and d are the coefficients, sig_{ld} represents the tank control signal, which compares the average temperature of the tank T_a to the temperature of the return water from buildings T_{return} . sig_{ld} also represents the tank control signal, which compares the average temperature of the tank to the temperature limit T_{limit} , and sig_{ld}^{pre} denotes the last-step signal. It is noteworthy that the coefficients a , b , c , and d are the variables used in the rule-based control strategies to determine the water flow ratios for peak shaving v_{ps} , and load shifting v_{ls} . The parametric rule-based strategies are optimized to maximize the overall performance.

The objective of the optimization included minimizing total operational cost as shown in Eq. (11), i.e., the sum of electricity cost and total heating operational cost.

$$P_{total_mon} = P_{hea_mon} + P_{ele_mon} \quad (11)$$

In this study, the optimization variables were the water flow ratio for peak shaving v_{ps} , and the water flow ratio for load shifting v_{ls} . The optimization was achieved through the exploration of optimal coefficients a , b , c , and d in the rule-based control strategies. The optimization method used was a hybrid global optimization method. This method integrated both Particle Swarm Optimization and Hooke-Jeeves

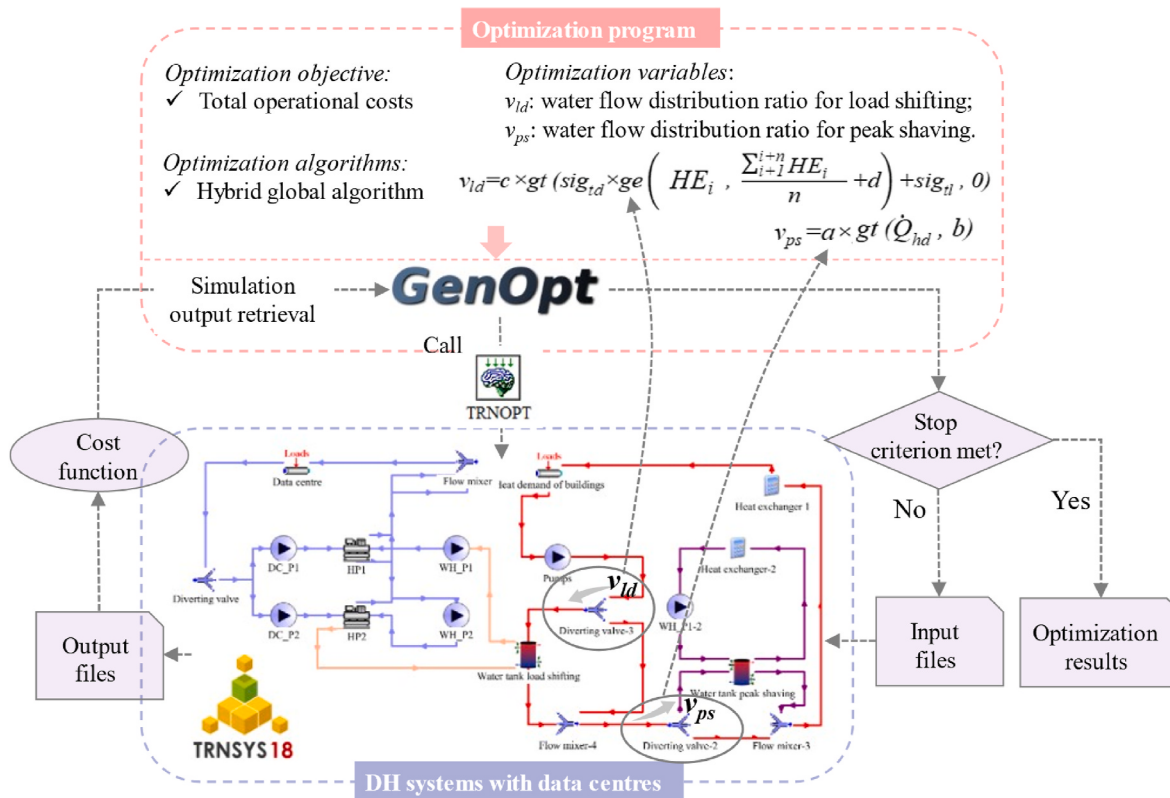


Fig. 4. Optimization using TRNSYS and GenOpt.

Generalized Pattern Search to achieve a balanced exploration of the entire solution space (global optimization) and the intensive exploitation of promising areas (local optimization) [58]. Particle Swarm Optimization was used to perform a global search and identify promising regions within the solution space. The best solution identified by Particle Swarm Optimization was then used as the initial guess of the Hooke-Jeeves method for local refinement. The Particle Swarm Optimization algorithm utilized a global best (gbest) neighborhood topology, with 12 particles evolving over 16 generations. Both the cognitive and social acceleration coefficients were set to 0.5. The maximum discrete velocity and constriction gain were also assigned a value of 0.5. For the Hooke-Jeeves method, the mesh size divider was set to 2, the initial mesh size exponent was 0, the mesh size exponent increment was 1, and the number of step reductions was 4. These settings were identified suitable for the optimization through trial-and-error testing. A detailed summary of the optimization variables is provided in Table 3.

3. Description of a case study and scenario design

3.1. Case study description

The performance of the proposed framework was assessed using the hybrid DH system on a university campus in Norway. Fig. 5 illustrates the topology of the campus DH network, which integrates waste heat from a DC. The system served various buildings on the campus, with a

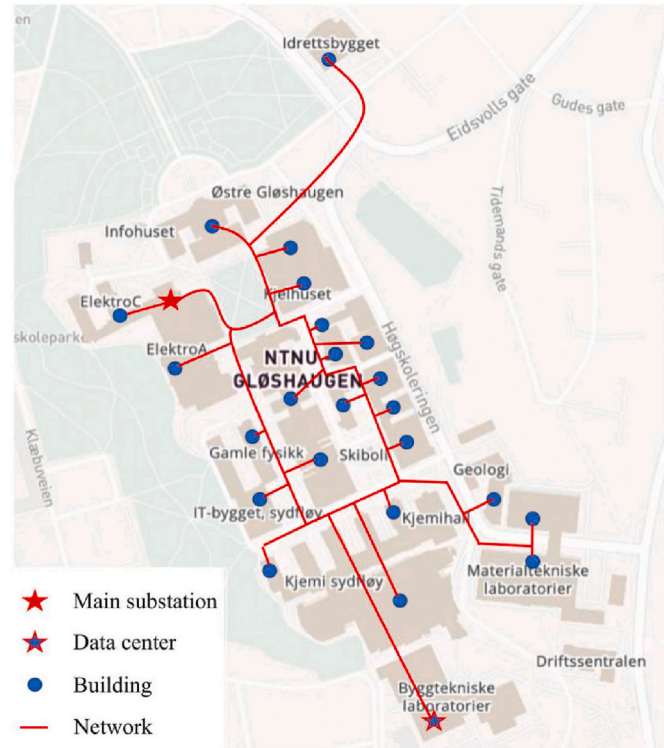


Fig. 5. Configuration of the campus DH network integrated with a DC [34].

total building area of approximately 300,000 m². For more detailed information about these buildings, please refer to the previous studies [34,59]. Over the course of a year, the DC contributed around 20 % of

Table 3
Range of optimization variables.

Variables	Initial value	Optimized range	Step size	Maximum iteration numbers
a	0.5	0–1	0.2	500
b	5000	3770–9400	1100	500
c	0.5	0–1	0.2	500
d	5	0–10	2	500

the heat required by the buildings, while the remaining 80 % was supplied by the city DH network through the main substation. Please note that this study focused on a campus-level DH system, rather than a city-level heating network.

The schematic of this hybrid DH system is illustrated in Fig. 6, which consists of a DC, two series-connected heat pumps, two water pumps, a main DH substation equipped with two heat exchangers, and a campus DH network.

There are two common methods for connecting DCs with DH networks: the return-to-supply (R2S) and the return-to-return (R2R) connection methods [60]. In this study, the R2R connection method was selected due to its suitability for the existing buildings and their temperature requirements, eliminating the need for additional heat sources to elevate the temperature of the water supplied to the DH system.

During the simulation process, the input file included day-ahead spot prices, the cooling energy from the DC, and the heating demand from campus buildings. The load data selected for this analysis corresponded to January 2018 with hourly observations. This period was chosen because January was in the middle of the heating season. Fig. 7 displays the measured cooling energy demand of the DC, the heating demand of the buildings, and the day-ahead spot prices. While the cooling energy demand exhibited a stable pattern, both the heating demand and spot prices showed significant fluctuations.

3.2. Scenario design

In this study, several scenarios were designed and compared to enhance the energy flexibility of the system. Fig. 8 presents the system configurations of different scenarios. In Scenario 1 (Fig. 8(a)), no water tanks were added to the system and this scenario was used as the baseline scenario. In Scenario 1, the return water from the building was heated up by the waste heat recovered from the DC and the city DH. This heated water was then redirected into the return water pipes to meet a proportion of building heating demand. In Fig. 8(b), a water tank was introduced to enhance energy flexibility through load shifting driven by real-time prices. This tank was charged using the waste heat recovered from the DC and the stored heat was discharged to the buildings when needed, by employing a moving average rule-based control strategy. In Fig. 8(c), a water tank was introduced to improve the system flexibility through peak shaving based on the instantaneous building heating demand. The tank was charged via a heat exchanger located in the main DH substation, utilizing a momentary rule-based control strategy. Fig. 8(d) combines the characteristics of Fig. 8(b) and (c), featuring two TES tanks for enhanced flexibility through both load shifting and peak shaving.

Scenario 1 was used as the baseline without using any water tanks.

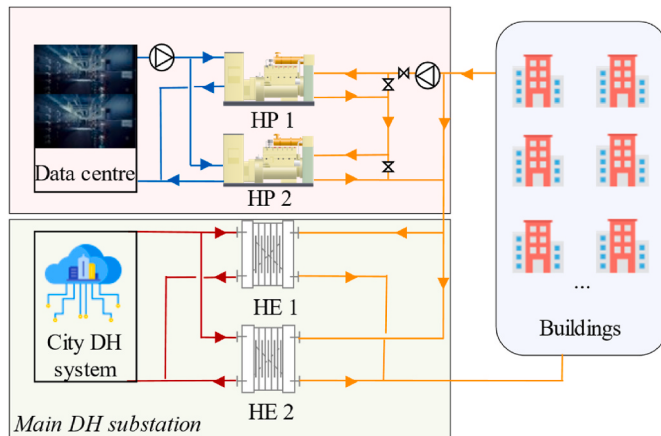


Fig. 6. The schematic of the hybrid DH system (HP is the heat pump, HE is the heat exchanger, and DH is the district heating).

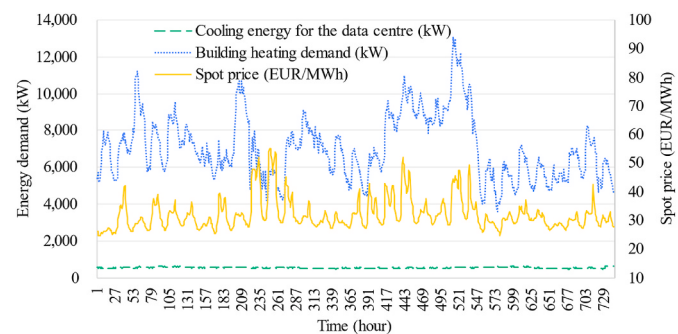


Fig. 7. Day-ahead spot prices and measured energy demand.

Scenario 2 included a water tank with a capacity of 600 m^3 for load shifting. Scenario 3 included a water tank with a capacity of 900 m^3 for peak shaving. Scenario 4 was a combination of Scenario 2 and Scenario 3, using two tanks with a capacity of 600 m^3 and 900 m^3 , respectively. Scenario 5 was an optimized version of Scenario 4 by using TRNOPT, addressing the suboptimal coefficients and setpoints in the rule-based control strategies used in Scenario 4. As two tanks with a total capacity of 1500 m^3 were used in Scenario 4 and Scenario 5 for both load shifting and peak shavings, another two scenarios with a single water tank of 1500 m^3 were designed for load shifting only (Scenario 6) and peak shaving only (Scenario 7).

The capacity of the water tanks plays a crucial role in enhancing the energy flexibility of the system. The size of water tanks may have a substantial influence on the overall performance of the system. Therefore, additional scenarios were designed to facilitate the comparison. Scenarios 8, 5, 9, and 10 were designed to use a water tank for peak shaving with a size of 600 m^3 , 900 m^3 , 1200 m^3 , and 1500 m^3 , respectively, while keeping the size of the water tank (600 m^3) for load shifting constant. Similarly, Scenarios 11, 5, 12, and 13 were designed to use a water tank for load shifting with a tank size of 300 m^3 , 600 m^3 , 900 m^3 , and 1200 m^3 , respectively, without altering the water tank size (900 m^3) for peak shaving. Table 4 summarizes the types of flexibility, sources, and control strategies employed in these different scenarios. The operational strategies used are in these scenarios as follows:

Strategy #1: waste heat generated by the DC was introduced into the return water from the buildings to meet a portion of the building heating demand.

Strategy #2: the water tank was charged with the waste heat collected from the DC. The charging or discharging of the water tank was driven by spot prices, using a moving average rule-based control strategy.

Strategy #3: the water tank was charged through one of the two heat exchangers in the DH substation and the second heat exchanger was used to increase the water temperature to the desired level. The charging and discharging processes were controlled by a setpoint related to building heating demand, using a momentary rule-based control strategy.

4. Results and discussion

In this section, the main results obtained from the performance testing and evaluation of the proposed framework are presented based on the case study presented in Section 3.

4.1. Performance comparison of the hybrid DH system with and without water tanks

Fig. 9 presents the overall system performance of Scenarios 2–4 that used water tanks for load shifting or peak shaving or both as compared to Scenario 1 without using any water tanks. In all three scenarios, the waste heat contributed approximately 10 % to building heating demand.

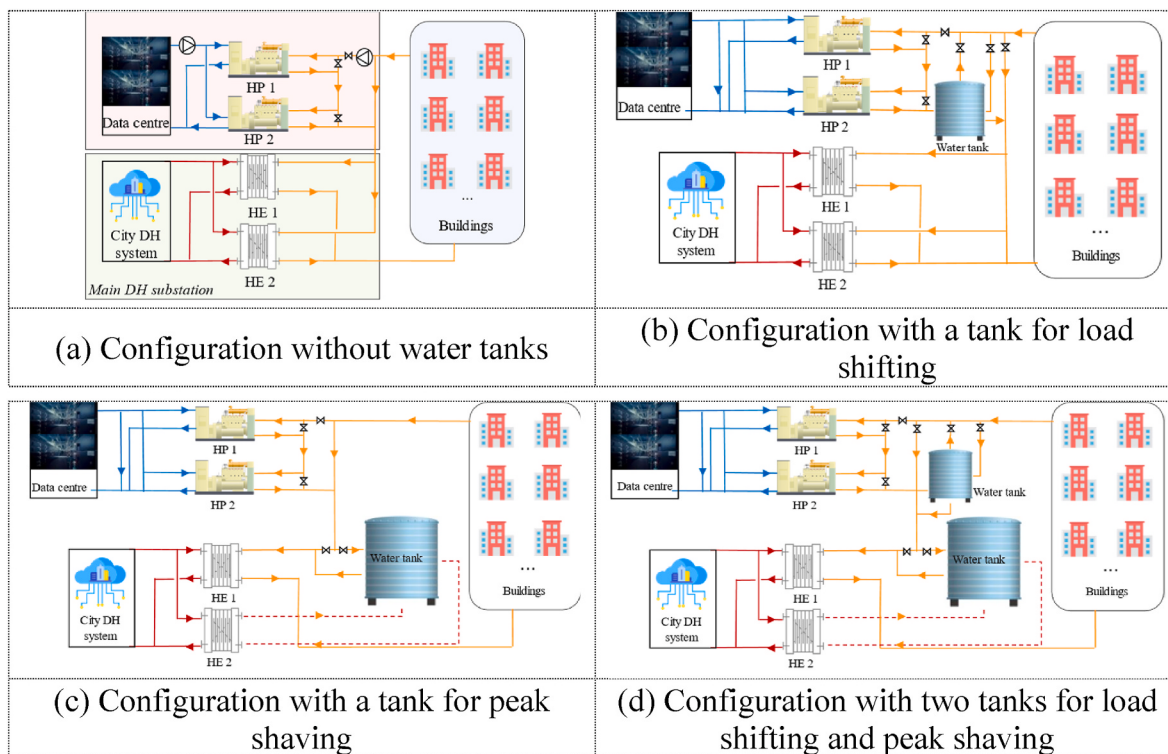


Fig. 8. Illustration of different configurations considered.

Table 4
Summary of flexibility types, sources, and control strategies used for each scenario.

Scenario No.	Flexibility type ^a	Waste heat	Tank size	Operational strategy
1	A	Yes	n/a	#1
2	A, B	Yes	600	#1, #2
3	A, C	Yes	900	#1, #3
4	A, B, C	Yes	600 (B) & 900 (C)	#1, #2, #3
5	A, B, C	Yes	600 (B) & 900 (C)	#1, #2, #3
6	A, B	Yes	1500	#1, #2
7	A, C	Yes	1500	#1, #3
8	A, B, C	Yes	600 (B) & 600 (C)	#1, #2, #3
9	A, B, C	Yes	600 (B) & 1200 (C)	#1, #2, #3
10	A, B, C	Yes	600 (B) & 1500 (C)	#1, #2, #3
11	A, B, C	Yes	300 (B) & 900 (C)	#1, #2, #3
12	A, B, C	Yes	900 (B) & 900 (C)	#1, #2, #3
13	A, B, C	Yes	1200 (B) & 900 (C)	#1, #2, #3

^a A: load covering; B: load shifting; C: peak shaving.

This value was dependent on the capacity of the DC and building heating demand. It should be noted that other than those particularly mentioned, the increases or reductions presented in the following sections were determined in comparison with Scenario 1.

In Scenario 2, a water tank with a size of 600 m³ was used for load shifting, leading to a 10 % decrease in the COP. This reduction was due to the elevated temperature of the water in the tank, which adversely affected the COP of the heat pumps. The load shifting capacity was approximately 2 %, while the peak shaving capacity was insignificant. As a result, the total costs were reduced by 1 % only in comparison to

Scenario 1.

In Scenario 3, a water tank of 900 m³ was used for peak shaving. The COP and electricity costs nearly remained unchanged compared to Scenario 1. This was attributed to that the water tank was connected to the heat exchangers for charging, rather than directly recovering the waste heat from the DC, as mentioned in Section 3. 2. As a result, the peak shaving approach had only a minor impact on the COP and electricity use of the heat pumps. The load shifting capacity was insignificant, while the peak reduction ratio improved by 7.5 %. Consequently, the total costs were reduced by 1.6 %.

Compared to the baseline, Scenario 4 which used two water tanks achieved a peak reduction ratio of 8 %, and a load shifting ratio of 1.9 %. As a result, the total costs were reduced by 2.5 %. The radar chart indicated that better overall performance was achieved under Scenario 4 by using dual TES when compared to Scenarios 2 and 3.

4.2. Performance evaluation of the optimized hybrid DH systems with water tanks

Based on the above analysis, although Scenario 4 demonstrated better performance than Scenarios 1–3, the parameter settings used in this scenario were not optimal. Therefore, Scenario 5 was an optimized version of Scenario 4 with the same size of the two water tanks by optimizing the parameter settings used in the rule-based control strategies. To be specific, the optimization was achieved by searching for the optimal values of the parameters including a , b , c , and d used in the rule-based strategies, which were linked with v_{ps} and v_{ls} , within the defined ranges to minimize the total operational cost of the system shown in Eq. (11) during the operation period. The simulation across the operation period was repeated multiple times, and each time, the optimizer tuned the parameter settings based on heuristics derived from the outcomes of the previous simulations, progressively approaching the optimal parameter settings.

The optimized results for the variables v_{ps} and v_{ls} were calculated using Eq. (6) and Eq. (7), respectively, in which a was 0.69, b was 6243 kW, c was 0.59, and d was 3.06 according to the optimization results.

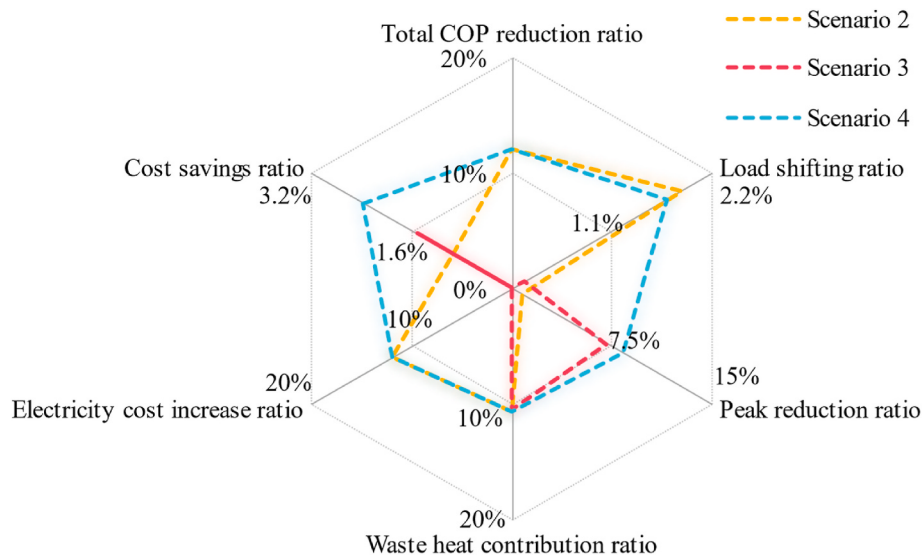


Fig. 9. Overall system performance under Scenarios 2–4.

The total operational costs of Scenario 5 were 198,417 EUR. From Fig. 10, it was discovered that compared to Scenario 1, the COP decreased by 15 % due to the high-temperature water in the water tank. The load shifting ratio was found to be 2.1 %, and the peak reduction ratio approached 10 %. Despite a 15 % increase in electricity costs, the total costs decreased by 3.2 %.

Fig. 10 also illustrates the performance differences across Scenarios 5, 6, and 7. It is important to note that the waste heat contribution ratio remained at approximately 10 % across these scenarios. This consistency was attributed to that the use of water tanks and demand response strategies did not significantly change the total waste heat recovered from the DCs, which accounted for around 10 % of building heating demand in the baseline scenario. The 10 % waste heat contribution referred specifically to January 2018. January fell within the mid-heating season, during which heating demand was significantly higher than other months, while the waste heat generated by the DC remained relatively stable. Consequently, the annual average proportion of waste heat contribution was expected to exceed 10 %.

From the comparison, it can be observed that Scenario 5 showed the best performance in cost savings, peak shaving, and load shifting, while

it also resulted in significant reductions in COP and increases in electricity costs. Scenarios 6 and 7 also showed potential in load shifting, peak shaving, and cost savings compared with the baseline scenario. Scenario 6 showed a higher load shifting ratio while a lower peak reduction ratio than Scenario 7. Scenario 7 did not affect the COP and electricity costs while achieving the other benefits including cost savings, load shifting, peak reduction, and waste heat contribution.

Fig. 11 illustrates the relationship between the average temperature of the tank and the COP of the system in Scenario 5. The data points showed a clear negative correlation, where the COP decreased as the tank temperature increased. The trendline was represented by Eq. (12).

$$y = -0.1806x + 18.2729 \quad (12)$$

This indicated that for every 1 °C increase in tank average temperature, the COP dropped by approximately 0.18. This trend suggested that the efficiency of the system diminished with the increase in the average tank temperatures, likely due to increased power consumption by the heat pumps. Therefore, maintaining and managing the tank temperature at lower levels could help optimize the COP and enhance overall system efficiency. It is also noted that the COP was calculated

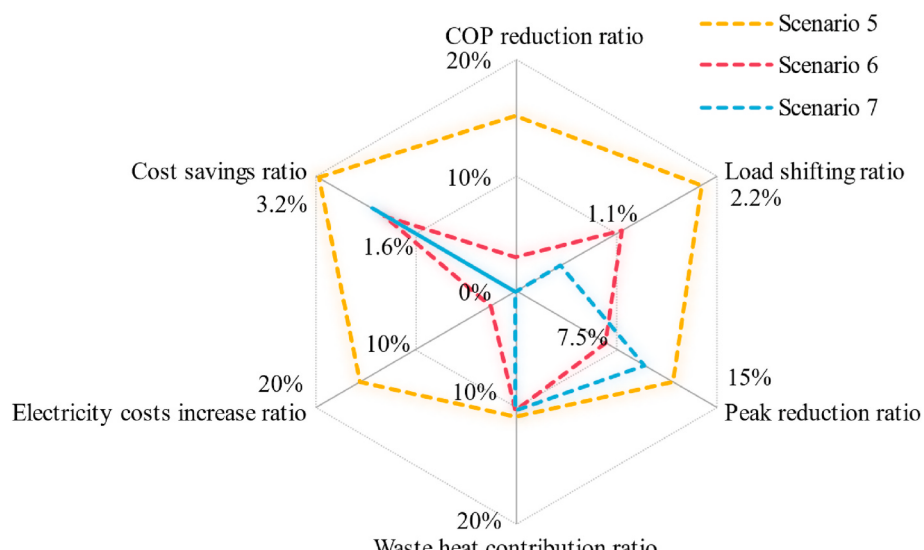


Fig. 10. Overall system performance under Scenarios 5–7.

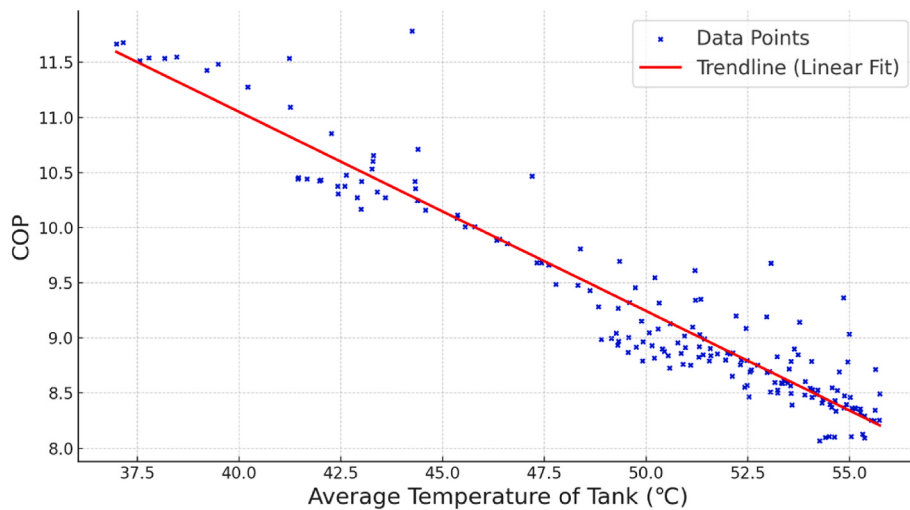


Fig. 11. Relationship between average temperature of the tank and COP.

using Eq. (1).

Peak shaving and load shifting can alter the momentary heating demand of buildings. To evaluate the effectiveness of the proposed rule-based control strategies, a one-week simulation was conducted. Fig. 12 illustrates the fluctuations in the building heating demand, the heat transfer rate from the heat exchangers at the DH substation for both Scenario 1 and Scenario 5, and the corresponding spot prices over a week's simulation. In Scenario 1, the heat transfer rate from the heat exchangers was lower than the building heating demand during most of the time due to the utilization of waste heat from the DC. In Scenario 5, the peak heat rate was notably lower than that in Scenario 1, highlighting the pivotal role of water tanks in peak shaving. Meanwhile, during the periods of peak heat demand and peak spot prices, both tanks worked together efficiently. Additionally, the results revealed that the heat transfer rate from the heat exchangers tended to be lower during the periods of the peak spot prices and tended to increase when the spot prices were lower. The simulation results demonstrated that the rule-based control strategies can effectively manage the charging and discharging of the water tanks.

As shown in Eq. (13), the CO₂ emission factor was used to calculate CO₂ emissions.

$$EM_{CO_2} = E \times EF \quad (13)$$

where EM_{CO_2} represents the CO₂ emissions, E is the heat or electricity use, and EF is the CO₂ emission factor for heat or electricity. The reference value for the CO₂ emission factor for heat was 51.8 g/kWh. Similarly, the reference value for the CO₂ emission factor for electricity was 18.9 g/kWh. For further details, please refer to Ref. [34].

Fig. 13 illustrates the CO₂ emissions under three conditions. In the baseline scenario, the chillers provided cooling energy for the DC, and the main substation supplied heat for building users, without waste heat recovery from the DC. As a result, the baseline scenario showed the highest CO₂ emissions due to a lack of waste heat utilization. Scenario 5 had slightly higher CO₂ emissions than Scenario 1. This increase was attributed to the need for storing heat in water tanks or the elevated tank temperatures, which led to lower COP of the heat pumps and higher electricity consumption. The CO₂ reduction or increase depended significantly on the calculation method. In this analysis, a constant coefficient was used to convert electricity and heat consumption into emissions.

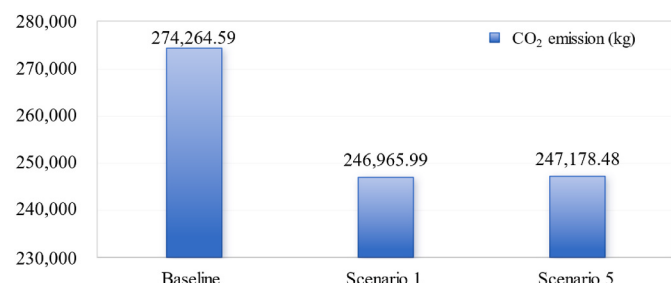


Fig. 13. CO₂ emissions of different scenarios.

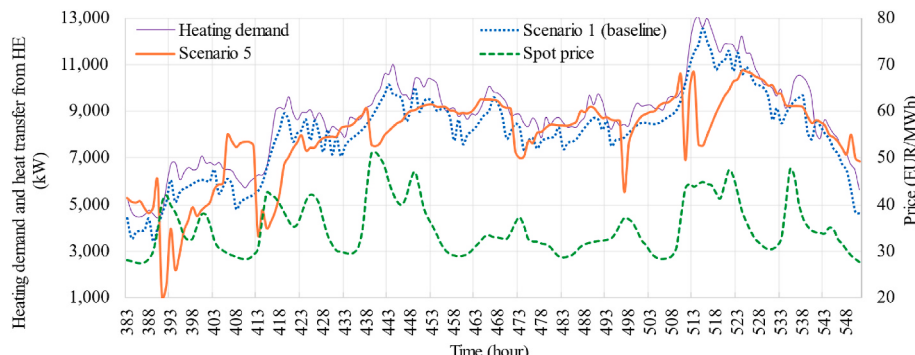


Fig. 12. Heat transfer from the heat exchangers of Scenario 1 and Scenario 5.

4.3. Impact of the water tank size on system performance

4.3.1. Evaluation of the impact of water tank size on peak shaving

In this section, the effect of the water tank size on the overall performance of the hybrid DH system was evaluated. Four different water tank sizes (i.e., 600 m³, 900 m³, 1200 m³, 1500 m³) were used for peak shaving while maintaining other parameters constant. It is noteworthy that this study concentrated on investigating the impact of the water tank size on the overall performance, and the initial investment and payback period of the water tanks were not considered, which have been explored in the previous studies [32,34].

Fig. 14 illustrates the results from Scenarios 5, 8, 9, and 10, focusing on the impact of varying water tank sizes for peak shaving. The analysis demonstrated that critical performance metrics, including COP, electricity costs, waste heat contribution, and load shifting capacity, remained relatively stable regardless of the changes in the water tank size. This was primarily due to the fact that the water tank used for peak shaving on the heat exchanger side showed a minor effect on the efficiency of the heat pumps, and therefore had a negligible impact on the COP and electricity costs. Waste heat contribution depended on the capacity of the DC and building demand. However, the results also revealed that the peak shaving ratio improved notably as the size of the water tanks increased.

4.3.2. Evaluation of the impact of water tank size on peak load shifting

Fig. 15 illustrates the performance of the hybrid DH system when using different water tank sizes (i.e. 300 m³, 600 m³, 900 m³, and 1200 m³) for load shifting while keeping all other parameters constant. It can be seen that the waste heat contribution was unaffected by the water tank size. The capacity for load shifting did not show a significant improvement when a larger water tank was used. Except for the use of a 300 m³ water tank, the load-shifting capacities using 600 m³, 900 m³, and 1200 m³ water tanks were similar and close to each other. Consequently, there was a negligible improvement in load shifting potential when increasing the size of the water tank.

5. Conclusion

This paper presented a novel framework for evaluating and enhancing the overall performance of DH systems integrated with DCs.

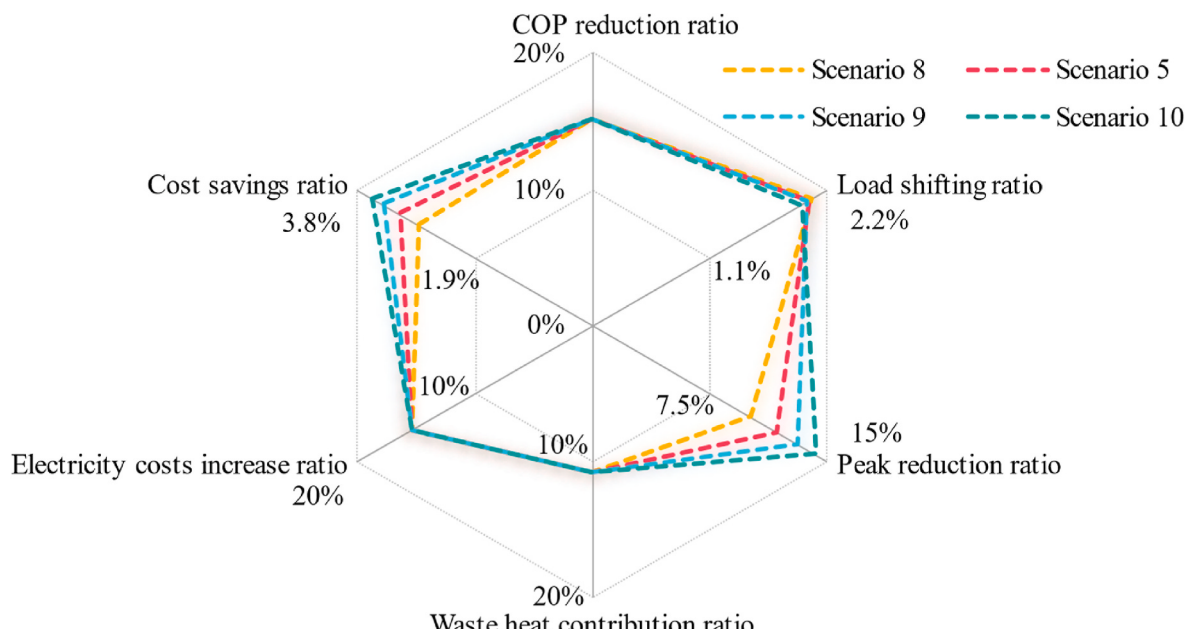


Fig. 14. Overall system performance when changing the size of the water tanks for peak shaving.

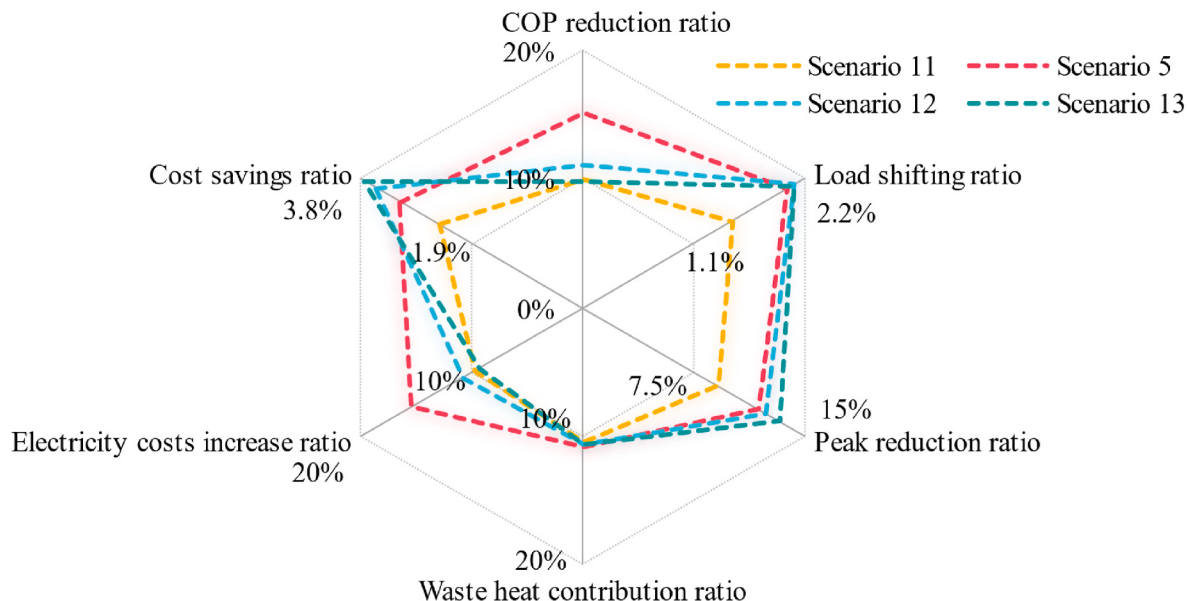


Fig. 15. System performance variation when changing the size of water tanks for load shifting.

CRediT authorship contribution statement

Han Du: Writing – original draft, Validation, Methodology, Investigation, Formal analysis, Conceptualization. **Xinlei Zhou:** Methodology. **Natasa Nord:** Writing – review & editing, Supervision, Resources. **Yale Carden:** Writing – review & editing, Supervision, Resources. **Ping Cui:** Writing – review & editing, Resources. **Zhenjun Ma:** Writing – review & editing, Supervision, Resources, Methodology.

Declaration of competing interest

The authors declare that they have no known competing financial interests or personal relationships that could have appeared to influence the work reported in this paper.

Acknowledgements

This work was partially supported by the LIFELINE-2050 project, funded by the Faculty of Engineering (IV) at the Norwegian University of Science and Technology (NTNU). The third author gratefully acknowledges the support of Green2050's partners and the encouragement of the innovation committee of IV faculty at NTNU.

Data availability

Data will be made available on request.

References

- [1] Reda F, Ruggiero S, Auvinen K, Temmes A. Towards low-carbon district heating: investigating the socio-technical challenges of the urban energy transition. *Smart energy* 2021;4:100054.
- [2] Luc KM, Heller A, Rode C. Energy demand flexibility in buildings and district heating systems – a literature review. *Adv Build Energy Res* 2018;13(2):241–63.
- [3] Yuan M, Vad Mathiesen B, Schneider N, Xia J, Zheng W, Sorkness P, et al. Renewable energy and waste heat recovery in district heating systems in China: a systematic review. *Energy* 2024;130788.
- [4] Vandermeulen A, van der Heijde B, Helsen L. Controlling district heating and cooling networks to unlock flexibility: a review. *Energy* 2018;151:103–15.
- [5] Mazhar AR, Liu S, Shukla A. A state of art review on the district heating systems. *Renew Sustain Energy Rev* 2018;96:420–39.
- [6] Lund H, Werner S, Wiltshire R, Svendsen S, Thorsen JE, Hvelplund F, et al. 4th generation district heating (4GDH). *Energy* 2014;68:1–11.
- [7] Gong Y, Ma G, Jiang Y, Wang L. Research progress on the fifth-generation district heating system based on heat pump technology. *J Build Eng* 2023;71.
- [8] Flynn C, Sirén K. Influence of location and design on the performance of a solar district heating system equipped with borehole seasonal storage. *Renew Energy* 2015;81:377–88.
- [9] Buffa S, Cozzini M, D'Antoni M, Baratieri M, Fedrizzi R. 5th generation district heating and cooling systems: a review of existing cases in Europe. *Renew Sustain Energy Rev* 2019;104:504–22.
- [10] von Rhein J, Henze GP, Long N, Fu Y. Development of a topology analysis tool for fifth-generation district heating and cooling networks. *Energy Convers Manag* 2019;196:705–16.
- [11] Meibodi SS, Loveridge F. The future role of energy geostructures in fifth generation district heating and cooling networks. *Energy* 2022;240.
- [12] Lake A, Rezaie B, Beyerlein S. Review of district heating and cooling systems for a sustainable future. *Renew Sustain Energy Rev* 2017;67:417–25.
- [13] Huang P, Copertaro B, Zhang X, Shen J, Löfgren I, Rönnelid M, et al. A review of data centers as prosumers in district energy systems: renewable energy integration and waste heat reuse for district heating. *Appl Energy* 2020;258.
- [14] Ebrahimi K, Jones GF, Fleischer AS. A review of data center cooling technology, operating conditions and the corresponding low-grade waste heat recovery opportunities. *Renew Sustain Energy Rev* 2014;31:622–38.
- [15] Khosravi A, Laukkonen T, Vuorinen V, Syri S. Waste heat recovery from a data centre and 5G smart poles for low-temperature district heating network. *Energy* 2021;218.
- [16] Tervo S, Syri S, Hiltunen P. Reducing district heating carbon dioxide emissions with data center waste heat – region perspective. *Renew Sustain Energy Rev* 2025;208.
- [17] Socci L, Rocchetti A, Verzino A, Zini A, Talluri L. Enhancing third-generation district heating networks with data centre waste heat recovery: analysis of a case study in Italy. *Energy* 2024;313.
- [18] Wahlroos M, Pärssinen M, Manner J, Syri S. Utilizing data center waste heat in district heating – impacts on energy efficiency and prospects for low-temperature district heating networks. *Energy* 2017;140:1228–38.
- [19] Pakere I, Goncarovs K, Grävelsiņš A, Zirne MA. Dynamic modelling of data center waste heat potential integration in district heating in Latvia. *Environ Energy* 2024;17(2).
- [20] Du H, Zhou X, Nord N, Carden Y, Ma Z. A new data mining strategy for performance evaluation of a shared energy recovery system integrated with data centres and district heating networks. *Energy* 2023;285.
- [21] Oró E, Taddeo P, Salom J. Waste heat recovery from urban air cooled data centres to increase energy efficiency of district heating networks. *Sustain Cities Soc* 2019;45:522–42.
- [22] Testasecca T, Catrini P, Beccali M, Piacentino A. Dynamic simulation of a 4th generation district heating network with the presence of prosumers. *Energy Convers Manag X* 2023;20.
- [23] Basciotti D, Judex F, Pol O, Schmidt R-R. Sensible heat storage in district heating networks: a novel control strategy using the network as storage. Conference: Sensible heat storage in district heating networks: a novel control strategy using the network as storage.
- [24] Kensby J, Trüschel A, Dalenbäck J-O. Potential of residential buildings as thermal energy storage in district heating systems–Results from a pilot test. *Appl Energy* 2015;137:773–81.
- [25] Guelpa E, Verda V. Thermal energy storage in district heating and cooling systems: a review. *Appl Energy* 2019;252.
- [26] Zhang Y, Johansson P, Kalagasisidis AS. Applicability of thermal energy storage in future low-temperature district heating systems – case study using multi-scenario analysis. *Energy Convers Manag* 2021;244.

- [27] Foteinaki K, Li R, Péan T, Rode C, Salom J. Evaluation of energy flexibility of low-energy residential buildings connected to district heating. *Energy Build* 2020;213.
- [28] Luc KM, Li R, Xu L, Nielsen TR, Hensen JLM. Energy flexibility potential of a small district connected to a district heating system. *Energy Build* 2020;225.
- [29] Sifnaios I, Sneum DM, Jensen AR, Fan J, Bramstoft R. The impact of large-scale thermal energy storage in the energy system. *Appl Energy* 2023;349:121663.
- [30] Gadd H, Werner S. Thermal energy storage systems for district heating and cooling. *Advances in thermal energy storage systems*. Elsevier; 2021. p. 625–38.
- [31] Olsthoorn D, Haghhighat F, Mirzaei PA. Integration of storage and renewable energy into district heating systems: a review of modelling and optimization. *Sol Energy* 2016;136:49–64.
- [32] Li H, Hou J, Tian Z, Hong T, Nord N, Rohde D. Optimize heat prosumers' economic performance under current heating price models by using water tank thermal energy storage. *Energy* 2022;239.
- [33] Pans MA, Claudio G, Eames PC. Theoretical cost and energy optimisation of a 4th generation net-zero district heating system with different thermal energy storage technologies. *Sustain Cities Soc* 2024;100.
- [34] Li H, Hou J, Hong T, Ding Y, Nord N. Energy, economic, and environmental analysis of integration of thermal energy storage into district heating systems using waste heat from data centres. *Energy* 2021;219.
- [35] Miedaner O, Mangold D, Sørensen PA. Borehole thermal energy storage systems in Germany and Denmark—Construction and operation experiences. Conference Borehole thermal energy storage systems in Germany and Denmark—Construction and operation experiences. p. 19–21..
- [36] Romanchenko D, Nyholm E, Odenberger M, Johnsson F. Impacts of demand response from buildings and centralized thermal energy storage on district heating systems. *Sustain Cities Soc* 2021;64.
- [37] Liu Z, Zhang Y, Zhang Y, Su C. Performance of a high-temperature transcritical pumped thermal energy storage system based on CO₂ binary mixtures. *Energy* 2024;305.
- [38] Zhang W, Ding J, Yin S, Zhang F, Zhang Y, Liu Z. Thermo-economic optimization of an artificial cavern compressed air energy storage with CO₂ pressure stabilizing unit. *Energy* 2024;294.
- [39] Péan TQ, Salom J, Ortiz J. Potential and optimization of a price-based control strategy for improving energy flexibility in Mediterranean buildings. *Energy Proc* 2017;122:463–8.
- [40] Hou J, Li H, Nord N, Huang G. Model predictive control for a university heat prosumer with data centre waste heat and thermal energy storage. *Energy* 2023; 267.
- [41] Verrilli F, Srinivasan S, Gambino G, Canelli M, Himanka M, Del Vecchio C, et al. Model predictive control-based optimal operations of district heating system with thermal energy storage and flexible loads. *IEEE Trans Autom Sci Eng* 2016;14(2): 547–57.
- [42] Awan MB, Sun Y, Lin W, Ma Z. A framework to formulate and aggregate performance indicators to quantify building energy flexibility. *Appl Energy* 2023; 349.
- [43] Yan X, Ozturk Y, Hu Z, Song Y. A review on price-driven residential demand response. *Renew Sustain Energy Rev* 2018;96:411–9.
- [44] Weck MHJ, van Hooff J, van Sark WGJHM. Review of barriers to the introduction of residential demand response: a case study in The Netherlands. *Int J Energy Res* 2017;41(6):790–816.
- [45] Eurelectric. Dynamic pricing in electricity supply. 2017.
- [46] research Ne. The development of district heating in the nordic countries. 2008.
- [47] Ewen M. European wholesale electricity price data. 2024.
- [48] Li H, Hou J, Nord N. Optimal design and operation for heat prosumer-based district heating systems. Conference Optimal design and operation for heat prosumer-based district heating systems..
- [49] Lygnerud K, Yang Y. Capturing flexibility gains by price models for district heating. *Energy* 2024;294.
- [50] Ding Y, Timoudas TO, Wang Q, Chen S, Brattelbø H, Nord N. A study on data-driven hybrid heating load prediction methods in low-temperature district heating: an example for nursing homes in Nordic countries. *Energy Convers Manag* 2022;269.
- [51] Ding Y, Ivanko D, Cao G, Brattelbø H, Nord N. Analysis of electricity use and economic impacts for buildings with electric heating under lockdown conditions: examples for educational buildings and residential buildings in Norway. *Sustain Cities Soc* 2021;74.
- [52] Zhang Z, Zhou X, Du H, Cui P. A new model predictive control approach integrating physical and data-driven modelling for improved energy performance of district heating substations. *Energy Build* 2023;301.
- [53] Alimohammadisagvand B, Jokisalo J, Kilpeläinen S, Ali M, Sirén K. Cost-optimal thermal energy storage system for a residential building with heat pump heating and demand response control. *Appl Energy* 2016;174:275–87.
- [54] Alimohammadisagvand B, Jokisalo J, Sirén K. Comparison of four rule-based demand response control algorithms in an electrically and heat pump-heated residential building. *Appl Energy* 2018;209:167–79.
- [55] Yang S. The simulation study of ground-source heat pump variable flow rate system based on TRNSYS. China, Shangdong: Shandong Jianzhu University; 2016.
- [56] Ferrara M, Fabrizio E, Virgone J, Filippi M. Energy systems in cost-optimized design of nearly zero-energy buildings. *Autom ConStruct* 2016;70:109–27.
- [57] Al-Alili A, Hwang Y, Radermacher R, Kubo I. Optimization of a solar powered absorption cycle under Abu Dhabi's weather conditions. *Sol Energy* 2010;84(12): 2034–40.
- [58] Wetter M. GenOpt generic optimization program, user manual version 3.1.1. 2016.
- [59] Guan J, Nord N, Chen S. Energy planning of university campus building complex: energy usage and coincidental analysis of individual buildings with a case study. *Energy Build* 2016;124:99–111.
- [60] Nord N, Shakerin M, Tereshchenko T, Verda V, Borchiellini R. Data informed physical models for district heating grids with distributed heat sources to understand thermal and hydraulic aspects. *Energy* 2021;222:119965.